Resonant photoelectron spectroscopy of Au2 via a Feshbach state using high-resolution photoelectron imaging

Iker León, Zheng Yang, and Lai-Sheng Wang

Citation: The Journal of Chemical Physics **139**, 194306 (2013); doi: 10.1063/1.4830408
View online: http://dx.doi.org/10.1063/1.4830408
View Table of Contents: http://scitation.aip.org/content/aip/journal/jcp/139/19?ver=pdfcov
Published by the AIP Publishing

Resonant photoelectron spectroscopy of Au_2^- via a Feshbach state using high-resolution photoelectron imaging

Iker León, Zheng Yang, and Lai-Sheng Wang[a)]
Department of Chemistry, Brown University, Providence, Rhode Island 02912, USA

(Received 6 October 2013; accepted 30 October 2013; published online 18 November 2013)

Photodetachment cross sections are measured across the detachment threshold of Au_2^- between 1.90 and 2.02 eV using a tunable laser. In addition to obtaining a more accurate electron affinity for Au_2 (1.9393 ± 0.0003 eV), we observe eight resonances above the detachment threshold, corresponding to excitations from the vibrational levels of the Au_2^- ground state ($X\ ^2\Sigma_u^+$) to those of a metastable excited state of Au_2^- (or Feshbach resonances) at an excitation energy of 1.9717 ± 0.0003 eV and a vibrational frequency of 129.1 ± 1.5 cm^{-1}. High-resolution photoelectron spectra of Au_2^- are obtained using photoelectron imaging to follow the autodetachment processes by tuning the detachment laser to all the eight Feshbach resonances. We observe significant non-Franck-Condon behaviors in the resonant photoelectron spectra due to autodetachment from a given vibrational level of the Feshbach state to selective vibrational levels of the neutral final state. Using the spectroscopic data for the ground states of Au_2^- ($X\ ^2\Sigma_u^+$) and Au_2 ($X\ ^1\Sigma_g^+$), we estimate an equilibrium bond distance of 2.53 ± 0.02 Å for the Feshbach state of Au_2^- by simulating the Franck-Condon factors for the resonant excitation and autodetachment processes. © *2013 AIP Publishing LLC*. [http://dx.doi.org/10.1063/1.4830408]

I. INTRODUCTION

Autodetachment is sometimes observed in anion photoelectron spectroscopy as a result of resonant absorption of the detachment photon by the anion to a temporary excited state embedded in the electron detachment continuum.[1,2] Autodetachment often leads to "non-Franck-Condon" behaviors and for pure direct electronic processes the final vibrational profiles are determined by the overlap between the autodetaching temporary anion state and the final neutral states. Additionally, it is possible that the anionic electronic state undergoes other mechanisms involving vibrational autodetachment, such as a "curve jumping" between the anion's excited state and the neutral. These processes were explained in detail by Simons[3] and first studied by Berry[4] for autoionization of molecular Rydberg states. Autodetaching resonances were first observed by Lineberger and co-workers in atomic anions and in small molecular anions.[5] Such temporary anion excited states can be either Feshbach resonances[6] or shape resonances.[7] Feshbach resonances are long-lived anion excited states, usually involving two-electron transitions, whereas shape resonances are short-lived anion states, which involve one-electron transition and are characterized by an angular momentum barrier. Both Feshbach resonances and shape resonances were observed initially in electron scattering experiments.[8,9] However, they can also be accessed optically via photoexcitation of anions with tunable lasers.[5,10,11]

In principle, the autodetachment processes can be followed by photoelectron spectroscopy (PES) upon optical excitation to an anion resonant state. However, very few resonant PES experiments have been performed deliberately because most anion PES experiments are done with fixed wavelength detachment lasers. The first resonant PES experiment was done by Johnson and co-workers on O_2^- via optical excitation to the $v = 12$ vibrational level of the $A\ ^2\Pi_u$ excited state of O_2^-, which is a Feshbach resonance.[12] Schiedt and Weinkauf performed resonant PES following optical excitations to both Feshbach resonances and shape resonances in the *p*-benzoquinone anion and observed significant variations of the observed Franck-Condon (FC) profiles.[13] But the complex resonant PES features prevented detailed spectral analyses. Resonant PES has also been performed for anions with very low electron binding energies upon infrared excitation of a selected vibrational mode of the anions.[14–16] Recently, resonant PES has been reported via higher vibrational levels of a dipole-bound state in phenoxide.[17]

We have built a high-resolution PE imaging system for the study of size-selected atomic clusters and reported initial vibrationally resolved PE spectra for Au_2^- and Au_4^-.[18,19] Au_2^- was chosen as our first study because of its well-known spectroscopy.[20–28] We reported a more accurate electron affinity (EA) of 1.9393 ± 0.0006 eV for Au_2 and our high-resolution PE spectra of Au_2^- were comparable or even better resolved in regard to that reported by Gantefor *et al.* using zero electron-kinetic-energy (ZEKE) spectroscopy.[22] In a separate experiment, Gantefor *et al.* reported sharp autodetachment resonances above the detachment threshold in the

a)E-mail: Lai-Sheng_Wang@brown.edu

photodetachment cross sections of Au_2^-.[29] These resonances were tentatively assigned as Feshbach resonances. The purpose of this article is to investigate the autodetachment processes following optical excitation to these resonances using our high-resolution PE imaging capability. We also performed photodetachment cross section measurement across the detachment threshold and obtained a more accurate EA for Au_2. Eight resonances were observed, originating from the ground and excited vibrational levels of the Au_2^- electronic ground state ($X\ ^2\Sigma_u^+$) to those of the Feshbach state of Au_2^-. Resonant PE spectra were measured following autodetachment from these temporary anion excited states. Significant non-Franck-Condon behavior was observed in comparison with the off-resonant PE spectra. Certain vibrational features in the resonant PE spectra were enhanced due to autodetachment from specific vibrational levels of the Feshbach state. The Feshbach state was determined to have an excitation energy of 1.9717 ± 0.0003 eV above the anion ground state, a vibrational frequency of 129.1 ± 1.5 cm^{-1}, and an equilibrium bond distance of 2.53 ± 0.02 Å.

II. EXPERIMENTAL METHODS

The laser vaporization supersonic cluster source and the time-of-flight mass spectrometer are similar to our magnetic-bottle apparatus, which were described in detail before.[30] A gold disk was used as the laser vaporization target with a helium carrier gas seeded with 10% argon, which was shown to produce relatively cold gold cluster anions previously.[31] Clusters formed inside the nozzle were entrained by the carrier gas and underwent a supersonic expansion. After a skimmer, anions from the collimated cluster beam were extracted perpendicularly into a time-of-flight mass spectrometer. The Au_2^- anion of current interest was mass-selected and focused into a collinear velocity-map imaging (VMI) system.[18,19] The VMI lens was based on the design by Suits and co-workers for ion imaging,[32] which was modified and optimized for photoelectron imaging. Photoelectrons were accelerated toward a position-sensitive detector with a 75 mm diameter micro-channel plate coupled to a phosphor screen and a charge-coupled device (CCD) camera. A National Instrument PXI-mainframe system was used to control the whole apparatus and for data acquisition. The tunable detachment radiation (222–709 nm, linewidth <0.3 cm^{-1}) was from a Continuum Sunlite OPO system pumped by an injection-seeded Continuum Powerlite laser. Typically, pulse energies of 150 μJ were used, although for the resonant photoelectron imaging pulse energies below 50 μJ/pulse were used to avoid saturation effects. A half-wave plate combined with a high-quality Glan-Laser polarizer was used to achieve a high degree of polarization parallel to the imaging detector plane. For the current work, photoelectron images were averaged with 50 000 to 200 000 laser shots before inverse-Abel transformation to obtain the three-dimensional (3D) electron distributions from the recorded two-dimensional (2D) images. This reconstruction was done by both the BASEX[33] and pBASEX[34] programs, which yielded similar results. The imaging system was calibrated using the known spectrum of Au^-.

III. RESULTS AND DISCUSSION

A. Photodetachment cross sections of Au_2^- in the 1.90–2.02 eV region

1. Observation of resonances: Autodetachment from a temporary excited state of Au_2^-

Gantefor *et al.* reported the photodetachment cross sections of Au_2^- in the 1.95 and 2.00 eV photon energy range, just above the detachment threshold, and observed eight resonances as sharp peaks on top of the nearly smooth total electron yields from the direct non-resonant detachment processes.[29] These peaks were interpreted as resonant excitations from the vibrational ground state and hot bands of Au_2^- to the vibrational levels of a temporary excited state of Au_2^- followed by autodetachment. We re-investigated the photodetachment cross sections of Au_2^- with slightly higher spectral resolution and in a broader photon energy range between 1.90 and 2.02 eV, covering the detachment threshold, as shown in Fig. 1. Photodetachment cross section measurements to determine EAs were pioneered by Lineberger and Woodward[35] and extensively used for organic radicals by Brauman and co-workers.[36,37] The method usually works well for species with s-wave detachment due to the Wigner threshold law. An increase of the electron yield is expected at the detachment threshold and at each vibrational level of the neutral. The onset of the electron signal at ~1.92 eV in Fig. 1 corresponds to a hot band transition from the Au_2^- anion. Our previous high-resolution PE imaging study showed that the vibrational temperature of Au_2^- was ~175 K under similar experimental conditions.[18] The step at 1.94 eV corresponds to the detachment threshold of Au_2^-, allowing us to determine a more accurate EA for Au_2 as 1.9393 ± 0.0003 eV (see the inset of Fig. 1). This EA value is consistent with our previous report of 1.9393 ± 0.0006 eV,[18] but the uncertainty is reduced by a factor of two.

Above the detachment threshold, in addition to the expected increase of the electron yield at the higher vibrational levels of Au_2 (labeled as $1 \leftarrow 0'$ and $2 \leftarrow 0'$ transitions), eight sharp peaks were observed and labeled as *a* to *h*. The positions of these peaks and their assignments, which agree well with those reported previously,[29] are given in Table I and shown in Fig. 2, where the vibrational levels of the Au_2^- ground electronic state are designated as v' and those of the anion excited states are designated as v'^*. The most intense peak *f* corresponds to the transition from the anion ground vibrational level to that of the excited state, defining an excitation energy of 1.9717 ± 0.0003 eV. The second most intense peak *h* represents the transition from the anion ground vibrational level to the $v'^* = 1$ level of the excited state, yielding a fundamental vibrational frequency for the Au_2^- excited state as 129.1 ± 1.5 cm^{-1}, in good agreement with the 128 ± 2 cm^{-1} value reported previously.[29] All the other resonant peaks are due to excitations from the vibrational hot bands of Au_2^- to different vibrational levels of the Au_2^- excited state (see Table I and Fig. 2). Peaks *a* and *c* were relatively weak, because they were originated from the $v' = 2$ and 3 hot bands of Au_2^-, respectively.

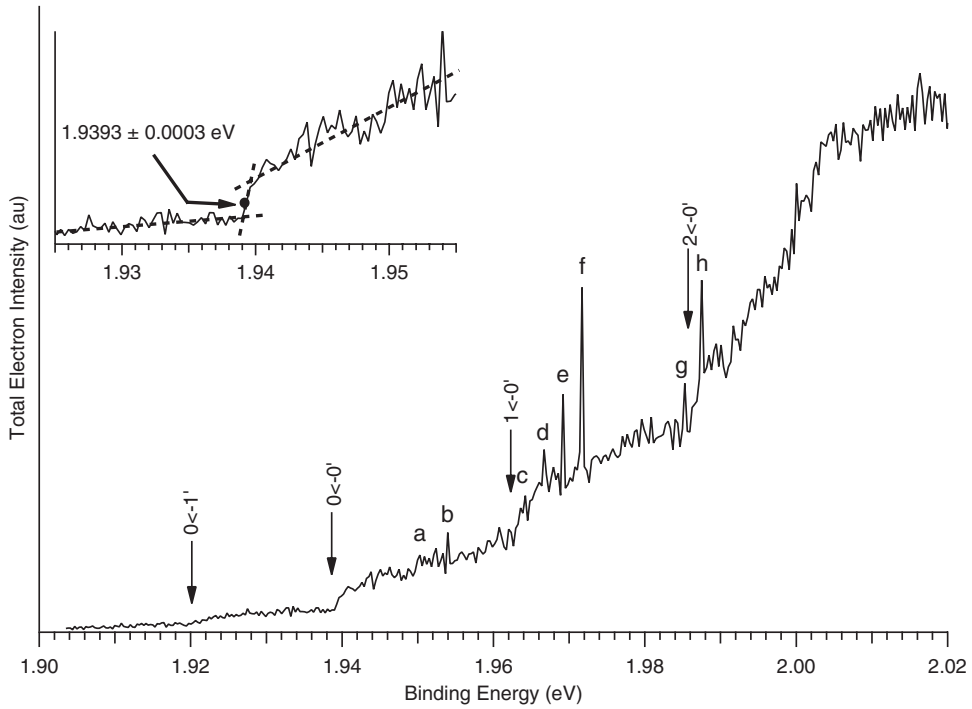

FIG. 1. Relative photodetachment cross sections of Au_2^- in the 1.90–2.02 eV region. The arrows show the transitions from the vibrational levels of the anion ground state to those of the neutral ground state. The peaks marked as, *a* to *h*, are resonances due to optical transitions from the anion ground state to an excited state of Au_2^- followed by autodetachment. The inset shows the detachment threshold of Au_2^- in more detail and how the electron affinity of Au_2 was evaluated.

2. Nature of the observed excited state of Au_2^-

The excited state observed for Au_2^- was tentatively assigned as a Feshbach resonance previously.[29] Autodetachment from such states results in relatively long lifetimes.[3,6] The resolution of the current photodetachment spectrum was higher than the previous measurement because the linewidth of our detachment laser (<0.3 cm^{-1}) was narrower than the previous experiment (~1 cm^{-1}).[29] Peak widths for the resonances in Fig. 1 were measured to be about 2.5 cm^{-1}, from which we estimated a lifetime of ~1.5 ps for the observed excited state of Au_2^-. This lifetime, which should be

TABLE I. The observed positions of the resonances in the photodetachment cross sections of Au_2^- (in both eV and cm^{-1}) in Fig. 1, their assignments as transitions from the Au_2^- vibrational levels (v′) to those (v′*) of the Au_2^- excited state (v′* ← v′),[29] autodetachment from the resonant state to the neutral Au_2 vibrational levels (v ← v′*), and the enhanced detachment transitions in the resonant PE spectra (v ← v′) in Fig. 4. The enhancement ratio refers to the ratio of the relative enhancement between two detachment transitions in the resonant PE spectra. This ratio provides a measure of the Franck-Condon factors of autodetachment transitions from the anion excited state (v′*) to the neutral vibrational levels (v). See text.

Observed peaks	Position (eV)	Position (cm^{-1})[a]	Resonant transition (v′* ← v′)	Autodetachment transitions (v ← v′*)	Enhanced PES transitions (v ← v′)	Enhancement ratio
a	1.9513	15738.3	1′* ← 2′	0 ← 1′* 1 ← 1′*	0 ← 2′ 1 ← 2′	$I_{0\leftarrow 1'^*/1\leftarrow 1'^*} = 0.8$[b]
b	1.9537	15757.3	0′* ← 1′	0 ← 0′* 1 ← 0′*	0 ← 1′ 1 ← 1′	$I_{0\leftarrow 0'^*/1\leftarrow 0'^*} = 2.3$
c	1.9644	15843.9	3′* ← 3′	0 ← 3′*	0 ← 3′	
d	1.9668	15863.3	2′* ← 2′	0 ← 2′* 1 ← 2′*	0 ← 2′ 1 ← 2′	$I_{0\leftarrow 2'^*/1\leftarrow 2'^*} = 0.9$[b]
e	1.9693	15883.5	1′* ← 1′	0 ← 1′* 1 ← 1′*	0 ← 1′ 1 ← 1′	$I_{0\leftarrow 1'^*/1\leftarrow 1'^*} = 2.6$
f	1.9717	15902.8	0′* ← 0′	0 ← 0′* 1 ← 0′*	0 ← 0′ 1 ← 0′	$I_{0\leftarrow 0'^*/1\leftarrow 0'^*} = 5.1$
g	1.9851	16010.9	2′* ← 1′	0 ← 2′* 1 ← 2′*	0 ← 1′ 1 ← 1′	$I_{0\leftarrow 2'^*/1\leftarrow 2'^*} = 2.6$
h	1.9877	16031.9	1′* ← 0′	0 ← 1′* 1 ← 1′*	0 ← 0′ 1 ← 0′	$I_{0\leftarrow 1'^*/1\leftarrow 1'^*} = 3.7$

[a]The uncertainty of the peak position is ±1.5 cm^{-1} and the uncertainty in relative peak intensity is ±25%.
[b]There is a larger uncertainty because of the relatively weak resonance.

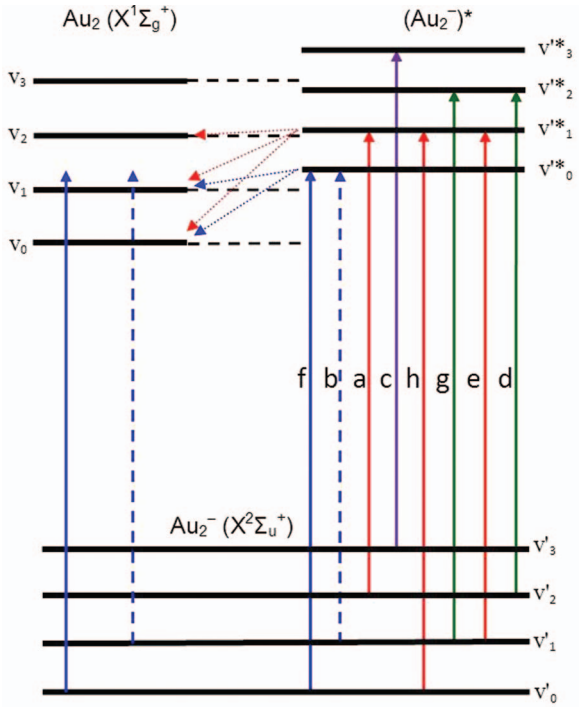

FIG. 2. Assignments of the vibrational transitions from the anion ground state ($X\ ^2\Sigma_u^+$) to the excited state of Au_2^- and the autodetachment from the excited state to the neutral ground state of Au_2 ($X\ ^1\Sigma_g^+$). The labels, *a* to *h*, designate optical transitions corresponding to those observed in Fig. 1.

viewed as a lower bound due to possible rotational broadening, is relatively long, consistent with the lifetimes estimated for the Feshbach resonances observed in the *p*-benzoquinone anion.[13]

The ground state of Au_2^- ($X\ ^2\Sigma_u^+$) has a $(d\sigma_g)^2(d\pi_u)^4(d\delta_g)^4(d\delta_u)^4(d\pi_g)^4(d\sigma_u)^2(s\sigma_g)^2(s\sigma_u)^1$ spin-free electron configuration, where the $s\sigma_g$ orbital represents the bonding highest occupied molecular orbital (HOMO) of neutral Au_2 and the $s\sigma_u$ orbital is the antibonding lowest unoccupied molecular orbital (LUMO) of neutral Au_2. Recent calculations on neutral Au_2 including spin-orbit coupling showed that the $d\pi_g$ orbital exhibits a large spin-orbit effect, so that the $d\pi_{1/2g}$ spinor is stabilized while the $d\pi_{3/2g}$ spinor is destabilized to become the HOMO.[28] The measured HOMO-LUMO gap from previous PES experiment of Au_2^- is 2.06 eV.[26] Thus, the observed excited state for Au_2^- is most likely the promotion of one $d\pi_{3/2g}$ HOMO electron to the $s\sigma_u$ LUMO to give a $(d\pi_{3/2g})^1(s\sigma_u)^2$ electron configuration. This is an allowed transition with an excitation energy of 1.9717 eV, as measured from the current experiment, which is very close to the HOMO-LUMO gap measured from the previous PES experiment.[26] The autodetachment then involves the following two-electron process: the emission of a $s\sigma_u$ electron and the transition of the other $s\sigma_u$ electron to the $d\pi_{3/2g}$ orbital, resulting in the ground state of Au_2. The relatively long lifetime of the excited state is consistent with the two-electron process, which is characteristic of Feshbach resonances. The detailed symmetry and nature of the anion excited state would deserve a more careful theoretical treatment.

3. Franck-Condon factor simulations between the Au_2^- ground state and the Feshbach state

Because the spectroscopic parameters and the vibrational temperature of the Au_2^- anion were well known from our recent high-resolution PES study,[18] FC simulations were carried out to estimate the equilibrium bond distance of the Feshbach state. The FC simulations were performed using the Pescal program,[38] which computes FC factors by numerical integration of vibrational wavefunctions of a Morse oscillator. Figure 3 shows the comparison between the intensities of the resonances in the detachment cross section spectrum with the simulated FC factors between the anion ground state and the Feshbach state at different equilibrium bond distances. The spectroscopic values employed are $\omega_e = 153\ cm^{-1}$,

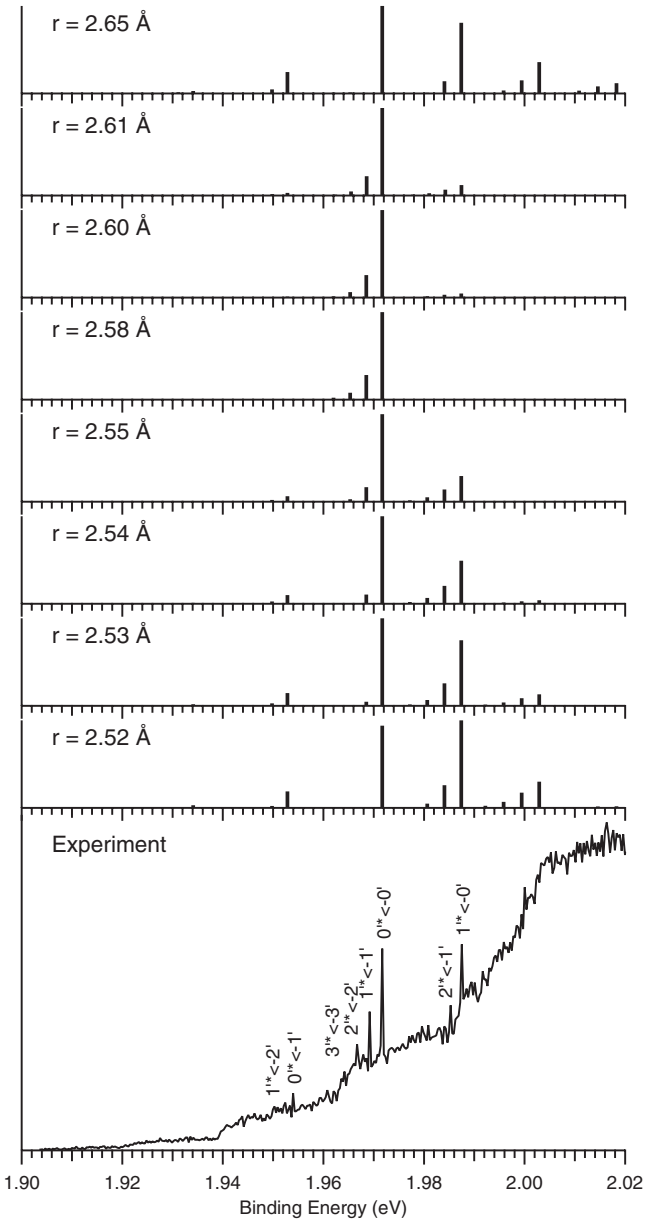

FIG. 3. Comparison of the calculated Franck-Condon factors, between the ground and excited states of Au_2^- at different excited state equilibrium bond distances, with the observed resonances in the photodetachment cross section spectrum (bottom).

$\omega_e x_e = 0.44\ cm^{-1}$, r = 2.587 Å, and a vibrational temperature of 175 K for the anion ground state from our recent study.[18] A frequency of 129.1 cm^{-1} was used for the Feshbach state with a guessed anharmonicity of 0.45 cm^{-1} (this value is not critical and does not affect the FC factors appreciably).

Since the vibrational frequency of the Feshbach state is slightly lower than the anion ground state, we started the FC simulation using bond lengths higher than that of the anion (2.587 Å).[18] As shown in Fig. 3, we found that at a bond distance of 2.61–2.62 Å (approximately +0.03 Å higher than the anion ground state) the simulated FC factors are in best agreement with the experimental intensity distribution of the observed resonant peaks in the detachment cross section spectrum. However, since the FC factors are only sensitive to the bond displacement, we found that at 2.55 Å, i.e., approximately 0.03 Å lower than the bond length of the anion ground state, good agreement with the experiment is also observed. Hence, these FC simulations cannot determine absolutely the equilibrium bond length of the Feshbach state, even though the vibrational frequency comparison seems to suggest a longer bond length. We will see below that the FC factors for the autodetachment from the Feshbach state to the neutral Au_2 ground state provide additional information that allows the equilibrium bond distance of the Feshbach state to be determined unequivocally.

B. Resonant photodetachment photoelectron imaging

To probe the autodetachment dynamics, we measured high-resolution photoelectron spectra by tuning the detachment laser to each of the eight Feshbach resonances, as shown in Fig. 4. The left column in Fig. 4 displays the resonant PE raw images and the converted PE spectra, where the labels (from *a* to *h*) correspond to the resonant peaks with the same labels in the photodetachment cross section spectrum in Fig. 1 and Table I. The right column in Fig. 4 shows the PE raw images and the converted PE spectra slightly off-resonance relative to the corresponding spectra in the left column for direct comparison. Each pair of the resonant and off-resonant PE images and spectra is plotted separately in Fig. S1 of the supplementary material.[39] The off-resonant spectra are similar to those we reported recently showing the direct detachment of the anion to the neutral continuum with a near threshold enhancement in each spectrum.[18] The resolved peaks represent vibrational features from the ground vibrational level and hot bands of the ground electronic state of Au_2^- ($X\ ^2\Sigma_u^+$) to the vibrational levels of the ground electronic state of neutral Au_2 ($X\ ^1\Sigma_g^+$). The assignments of the vibrational transitions are given in the 1.9875 eV spectrum. Because of the low detachment photon energies, only the first few vibrational features are observed for the broad Franck-Condon envelope of the Au_2 ($X\ ^1\Sigma_g^+$) ← Au_2^- ($X\ ^2\Sigma_u^+$) transition.[18] The resonant spectra consist of contributions from both direct detachment and autodetachment from the Feshbach state, resulting in enhancement in certain transitions governed by the Franck-Condon factors between the Feshbach resonances and the neutral final vibrational levels. The autodetachment transitions that lead to obvious enhancement are labeled in the resonant PE spectra in Fig. 4 and are also listed in Table I. The arrows in the off-resonant spectra indicate the peaks that are enhanced in the resonant spectra.

The autodetachments from the current Feshbach resonances are quite different from those observed recently from a dipole-bound state.[17] In the latter, because the structure of the molecular core of the dipole-bound state and the neutral structure are nearly identical, a $\Delta v = 1$ propensity was observed in the autodetachment from a given vibrational level of the dipole-bound state.

1. Assignments of the resonantly enhanced vibrational transitions

The enhanced vibrational peaks in the resonant PE spectra can be readily understood, as schematically shown in Fig. 2. For example, the resonance at 1.9717 eV (peak *f* in Fig. 1) represents the vibrational transition from the ground vibrational level of Au_2^- ($v' = 0$) to the ground vibrational level of the Feshbach state ($v'^* = 0$), which can autodetach to the $v = 0$ and $v = 1$ vibrational levels of neutral Au_2 (see Fig. 2). Hence, the corresponding vibrational features ($0 \leftarrow 0'$ and $1 \leftarrow 0'$) are enhanced in the resonant PE spectrum (Fig. 4(f)). The enhancement of the $0 \leftarrow 0'$ transition is much more pronounced, probably due to a large FC factor between the $v'^* = 0$ level of the Feshbach state and the $v = 0$ level of the neutral. The ratio of the enhancement between the $0 \leftarrow 0'$ and the $1 \leftarrow 0'$ transitions represents the ratio of the FC factors between the $0 \leftarrow 0'^*$ and $1 \leftarrow 0'^*$ autodetachment transitions, and it is given in Table I in the last column as $I_{0\leftarrow 0'^*/1\leftarrow 0'^*}$ (= 5.1). The resonance at 1.9537 eV (peak *b*) also reaches the $v'^* = 0$ level of the Feshbach state from the $v' = 1$ hot band of Au_2^- (Fig. 2). Hence, the $0 \leftarrow 1'$ and $1 \leftarrow 1'$ transitions are enhanced in the resonant PE spectrum (Fig. 4(b)). The ratio of the enhancement between these two peaks should be the same as that in Fig. 4(f). But we measured an enhancement ratio of only 2.3 (Table I), about a factor of 2 smaller than in the case of Fig. 4(f), reflecting the uncertainty in measuring relative peak intensities. The enhanced peaks in all the other resonant PE spectra in Fig. 4 can be understood similarly using the energy level diagram of Fig. 2. Basically, the enhanced peaks in the resonant PE spectra are governed by the FC factors between the vibrational levels of the Feshbach state and the neutral vibrational levels. The enhancement ratios can be used to compare with FC factor calculations for the autodetachment processes to provide another estimate for the equilibrium bond length of the Feshbach state.

2. Simulations of FC factors between the Feshbach state and the neutral ground state

As will be discussed below, the potential energy curves of the Feshbach state and the neutral in the current system intersect and thus the electron detachment can be understood by a mixture of electronic detachment process (involving anion-neutral Franck-Condon factors) and vibrational autodetachment process (non-Franck-Condon terms).[3] The latter can be particularly important when the kinetic energy of the detached electrons is small such that the de Broglie wavelength is of

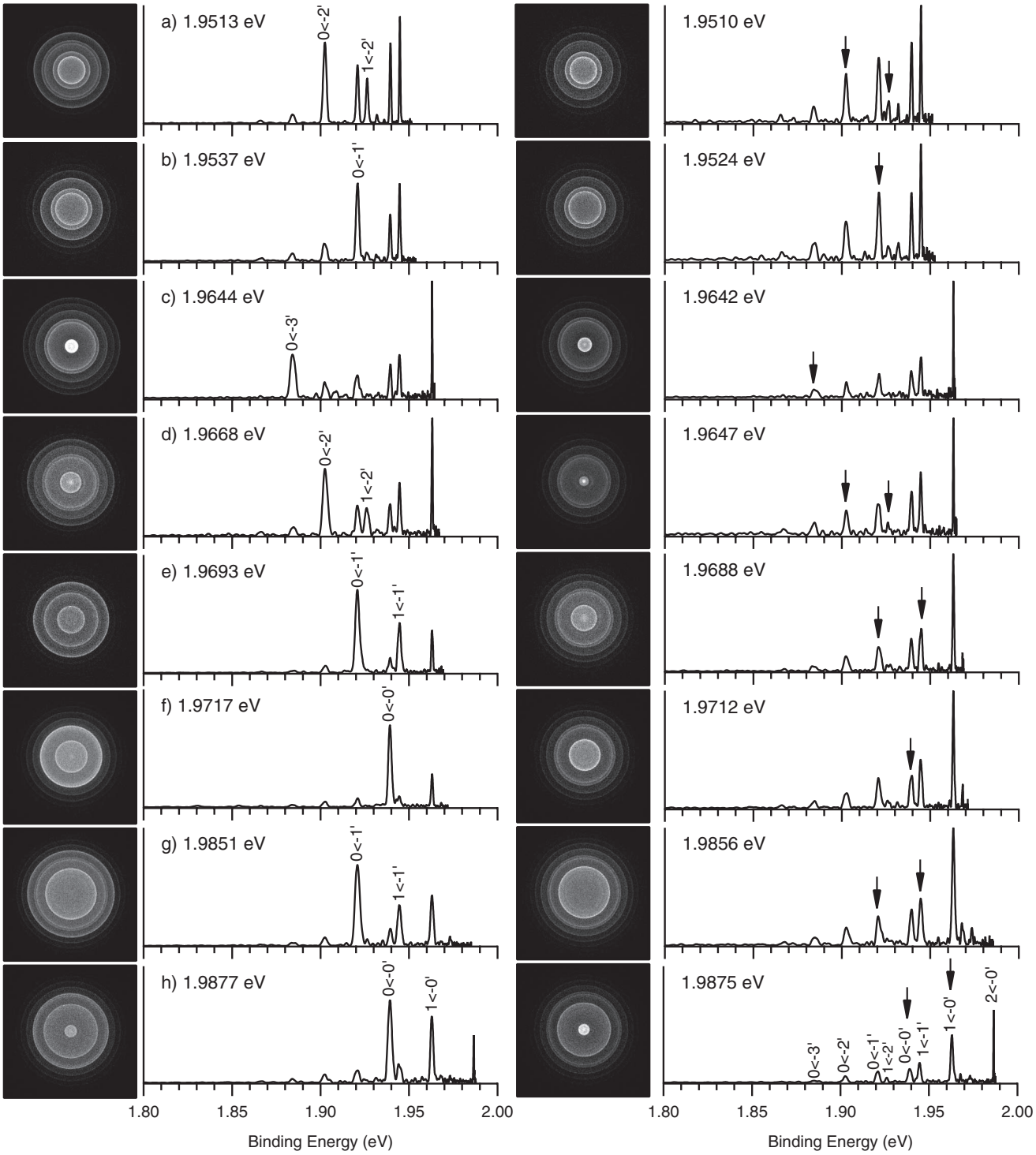

FIG. 4. Left panel: photoelectron images and spectra of Au_2^- at the eight resonances observed in Fig. 1, (a) 1.9513 eV, (b) 1.9537 eV, (c) 1.9644 eV, (d) 1.9668 eV, (e) 1.9693 eV, (f) 1.9717 eV, (g) 1.9851 eV, and (h) 1.9877 eV. Right panel: off-resonant PE images and spectra (by just a couple of meV or less) for direct comparison to the resonant spectra of the left panel. The arrows indicate the peaks that are obviously enhanced in the resonant spectra (labeled). The photoelectron images are raw images, which show better the resonant enhancement. The polarization of the detachment laser is vertical along the images. All detachment channels have isotropic angular distributions.

the order of the anion's HOMO radial extent. In the current work, we assume that the autodetachment is purely governed by the electronic process, which seems to be consistent with the observed vibrational enhancement. Using the ratio of the FC factors between the $0 \leftarrow 0'^*$ and $1 \leftarrow 0'^*$ autodetachment transitions deduced above from the resonant PE spectra, we can also estimate the equilibrium bond distance of the Feshbach state. Figure 5 compares the experimental FC factors of these two autodetachment transitions to simulations at various bond distances consistent with those in Fig. 3 for the Feshbach state. The simulations were done again using the Pescal program[38] and the spectroscopic parameters used for the Au_2

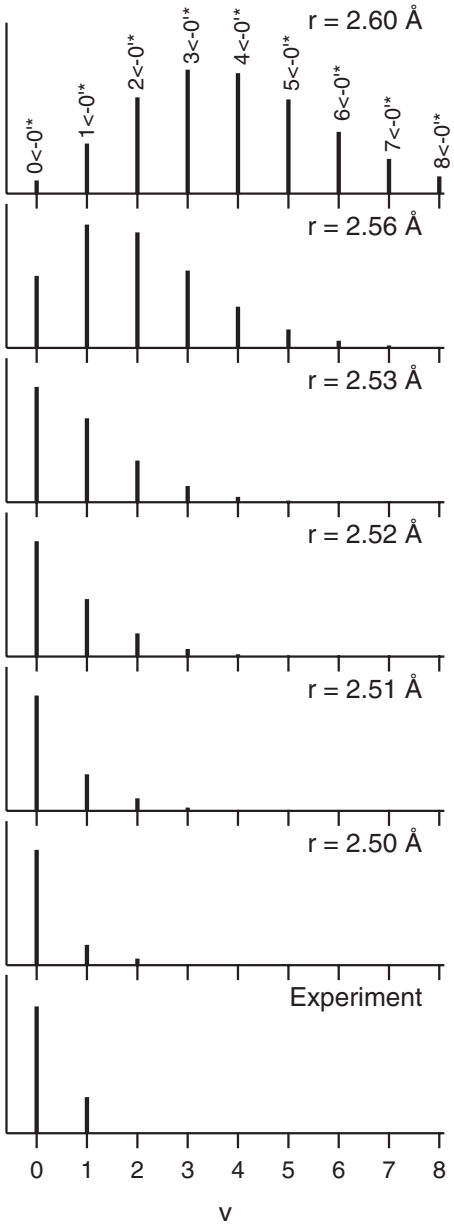

FIG. 5. Franck-Condon factors for the autodetachment transitions between the $v'^* = 0$ level of the Feshbach state to the neutral ground state at different anion excited state equilibrium bond distances. The bottom frame shows the observed ratio of the autodetachment transition strength to the v = 0 and v = 1 levels of the neutral.

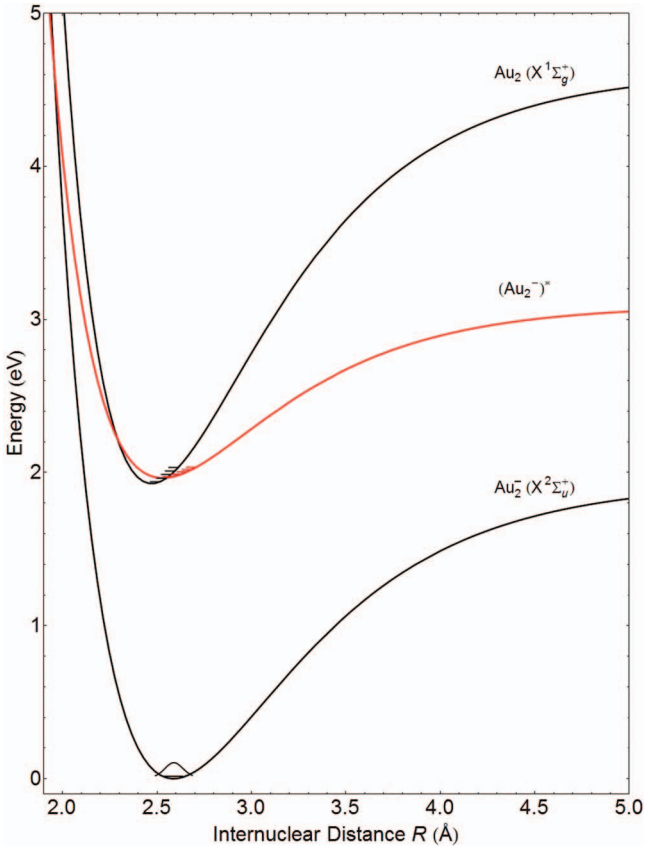

FIG. 6. Schematic Morse potential energy curves for the ground state of Au_2^- ($X\ ^2\Sigma_u^+$), the Feshbach state of Au_2^- (in red) and the neutral Au_2 ground state ($X\ ^1\Sigma_g^+$).

neutral ground state are as follows:[18] $\omega_e = 190.9\ cm^{-1}$, $\omega_e x_e = 0.42\ cm^{-1}$, r = 2.4715 Å. Figure 5 shows that when the bond distance of the Feshbach state is set to 2.60 Å, the FC factor of the $1 \leftarrow 0'^*$ transition is about 4 times more favorable than that for the $0 \leftarrow 0'^*$ transition, clearly inconsistent with the experiment. In fact, a bond distance larger than 2.61 Å leads to an almost negligible FC factor for the $0 \leftarrow 0'^*$ transition. A good match between the predicted FC factors and the experiment is found when the equilibrium distance is in the range between 2.51 and 2.54 Å, considering the experimental uncertainty. Combining with the result from Fig. 3, we estimated an equilibrium bond distance for the Feshbach state as 2.53 ± 0.02 Å, which also gives reasonable simulated FC factors for autodetachment from other resonant levels in comparison with the experiment. Hence, the equilibrium bond distance of the Feshbach state is slightly shorter than that of the anion ground state.

This result is conceivable, considering the electronic configuration suggested for the Feshbach state $[(d\pi_{3/2g})^1(s\sigma_u)^2]$. Since both the $d\pi_{3/2g}$ and $s\sigma_u$ orbitals are antibonding, the promotion of an electron from one to the other should not affect the Au–Au bonding significantly. In fact, our current result suggests that the $d\pi_{3/2g}$ orbital may be slightly more antibonding than the $s\sigma_u$ orbital, thus resulting in a slight shortening of the equilibrium bond distance when one $d\pi_{3/2g}$ electron is promoted to the $s\sigma_u$ orbital in the Feshbach state. It should be pointed out that the current result assumes that the real potential energy curves can be described by the Morse potential. The schematic Morse potential for the Feshbach state of Au_2^- is shown in Fig. 6, using the spectroscopic parameters obtained in this work, along with those for the anion and neutral ground states. The shorter equilibrium bond length and the lower vibrational frequency of the Feshbach state, in comparison to the Au_2^- ground state, may suggest a possible avoided curve crossing. It would be really interesting to consider the excited states of the Au_2^- anion using *ab initio* calculations.

IV. CONCLUSIONS

Eight autodetachment resonances were observed slightly above the detachment threshold of Au_2^-, which are attributed

to vibrational excitations from the anion ground vibrational level and hot bands to the vibrational levels of an anion excited state (or a Feshbach state). High-resolution photoelectron spectra of the Au_2 ($X\ ^1\Sigma_g^+$) ← Au_2^- ($X\ ^2\Sigma_u^+$) detachment transition were obtained at each of the eight Feshbach resonances. In comparison to the non-resonant spectra, we observed pronounced enhancement of certain vibrational peaks in the resonant PE spectra, governed by the Franck-Condon factors between the Feshbach state and the neutral ground state. New photodetachment cross section measurement provided a more accurate electron affinity (1.9393 ± 0.0003 eV) for Au_2. The Feshbach state was measured to be at 1.9717 ± 0.0003 eV above the ground state of the anion with a vibrational frequency of 129.1 ± 1.5 cm^{-1}. Franck-Condon simulations for the excitation to the Feshbach state and for the autodetachment from the Feshbach state to the neutral state yielded an estimated equilibrium bond distance of 2.53 ± 0.02 Å for the excited state of Au_2^-.

ACKNOWLEDGMENTS

I.L. would like to thank the Basque Government for a postdoctoral fellowship. This work was supported by the National Science Foundation (Grant No. CHE-1049717).

[1]S. M. Casey and D. G. Leopold, J. Phys. Chem. **97**, 816 (1993).
[2]J. Li, X. Li, H. J. Zhai, and L. S. Wang, Science **299**, 864 (2003).
[3]J. Simons, J. Am. Chem. Soc. **103**, 3971 (1981); in *Photoionization and Photodetachment*. Part II, edited by C. Y. Ng (World Scientific, Singapore, 1999), Chap. 17, pp. 958–1010.
[4]R. S. Berry, J. Chem. Phys. **45**, 1228 (1966).
[5]T. A. Patterson, H. Hotop, A. Kasdan, D. W. Norcross, and W. C. Lineberger, Phys. Rev. Lett. **32**, 189 (1974); S. E. Novick, P. L. Jones, T. J. Mulloney, and W. C. Lineberge, J. Chem. Phys. **70**, 2210 (1979); P. L. Jones, R. D. Mead, B. E. Kohler, S. D. Rosner, and W. C. Lineberger, *ibid.* **73**, 4419 (1980).
[6]C. Chin, R. Grimm, P. Julienne, and E. Tiesinga, Rev. Mod. Phys. **82**, 1225 (2010).
[7]M. N. Piancastelli, J. Electron Spectrosc. Relat. Phenom. **100**, 167 (1999).
[8]I. Shimamura and K. Takayanagi, *Electron-Molecule Collisions* (Plenum, New York, 1984), p. 382.
[9]G. J. Schultz, Rev. Mod. Phys. **45**, 423 (1973).
[10]C. G. Bailey, C. E. H. Dessent, M. A. Johnson, and K. H. Bowen, J. Chem. Phys. **104**, 6976 (1996).
[11]C. E. H. Dessent, J. Kim, and M. A. Johnson, Faraday Discuss. **115**, 395 (2000).
[12]C. G. Bailey, D. J. Lavrich, D. Serxner, and M. A. Johnson, J. Chem. Phys. **105**, 1807 (1996).
[13]J. Schiedt and R. Weinkauf, J. Chem. Phys. **110**, 304 (1999).
[14]C. L. Adams, H. Schneider, K. M. Ervin, and J. M. Weber, J. Chem. Phys. **130**, 074307 (2009).
[15]C. L. Adams, H. Schneider, and J. M. Weber, J. Phys. Chem. A **114**, 4017 (2010).
[16]C. L. Adams, B. J. Knurr, and J. M. Weber, J. Chem. Phys. **136**, 064307 (2012).
[17]H. T. Liu, C. G. Ning, D. L. Huang, P. D. Dau, and L. S. Wang, Angew. Chem., Int. Ed. **52**, 8976 (2013).
[18]I. León, Z. Yang, and L. S. Wang, J. Chem. Phys. **138**, 184304 (2013); Erratum: **139**, 089903 (2013).
[19]Z. Yang, I. León, and L. S. Wang, J. Chem. Phys. **139**, 021106 (2013).
[20]M. D. Morse, Chem. Rev. **86**, 1049 (1986).
[21]J. Ho, K. Ervin, and W. C. Lineberger, J. Chem. Phys. **93**, 6987 (1990).
[22]G. F. Gantefor, D. M. Cox, and A. Kaldor, J. Chem. Phys. **93**, 8395 (1990).
[23]B. Simard and P. A. Hackett, J. Mol. Spectrosc. **142**, 310 (1990).
[24]G. A. Bishea and M. D. Morse, J. Chem. Phys. **95**, 5646 (1991).
[25]A. M. James, P. Kowalczyk, B. Simard, J. C. Pinegard, and M. D. Morse, J. Mol. Spectrosc. **168**, 248 (1994).
[26]H. J. Zai, B. Kiran, and L. S. Wang, J. Chem. Phys. **121**, 8231 (2004).
[27]W. S. Hopkins, S. M. Hamilton, P. D. McNaughter, and S. R. Mackenzie, Chem. Phys. Lett. **483**, 10 (2009).
[28]K. R. Geethalakshmi, F. Ruiperez, S. Knecht, J. M. Ugalde, M. D. Morse, and I. Infante, Phys. Chem. Chem. Phys. **14**, 8732 (2012).
[29]G. F. Gantefor, D. M. Cox, and A. Kaldor, J. Chem. Phys. **94**, 854 (1991).
[30]L. S. Wang, H. S. Cheng, and J. W. Fan, J. Chem. Phys. **102**, 9480 (1995).
[31]W. Huang and L. S. Wang, Phys. Rev. Lett. **102**, 153401 (2009).
[32]D. Townsend, M. P. Minitti, and A. G. Suits, Rev. Sci. Instrum. **74**, 2530 (2003).
[33]V. Dribinski, A. Ossadtchi, V. A. Mandelshtam, and H. Reisler, Rev. Sci. Instrum. **73**, 2634 (2002).
[34]G. A. Garcia, L. Nahon, and I. Powis, Rev. Sci. Instrum. **75**, 4989 (2004).
[35]W. C. Lineberger and B. W. Woodward, Phys. Rev. Lett. **25**, 424 (1970).
[36]A. H. Zimmerman and J. I. Brauman, J. Chem. Phys. **66**, 5823 (1977).
[37]R. L. Jackson, P. C. Hiberty, and J. I. Brauman, J. Chem. Phys. **74**, 3705 (1981).
[38]K. M. Ervin, PESCAL, Fortran program, 2010.
[39]See supplementary material at http://dx.doi.org/10.1063/1.4830408 for the photoelectron images and spectra for each resonant vs. off-resonance comparison.